A Study on the Chemical and Thermal Stability and Mechanical Properties of Nanocrystallization on Zr-4 Alloy Surface Based on Mechanical Lapping

Mengxiong Lu[a], Qingze Zou[b]

[a]School of Electronics and Electrical Engineering, Changzhou College of Information Technology, Changzhou 213164, China.
[b]Department of Mechanical and Aerospace Engineering, Rutgers, the State University of New Jersey, Piscataway, NJ 08854, United States
njlmx9718@126.com

The nanocrystallization of the surface of industrial Zr-4 alloy is realized by means of the mechanical lapping technology. XRD diffractometer and transmission electron microscopy are applied to analyze the grain size, the micro-hardness and the micro-structure of Zr-4 alloy at different annealing temperatures. Meanwhile, a X-ray stress gauge is adopted to measure the stress properties of Zr-4 alloy. The results have indicated that mechanical lapping technology can effectively realize the surface nanocrystallization of industrial zirconium, and Zr-4 alloy can form a gradient nanometer crystal structure on its surface after mechanical lapping. After SMAT processing, the diffraction characteristics of Zr-4 alloy have experienced significant changes. The grain orientation has transformed in the process of SMAT treatment and the diffraction peak intensity of the sample changes with the increase of SMAT treatment time. The size of the grain on the alloy surface tends to decrease first and then increase. When the treatment time is 15mins, the grain size reaches a minimum value of 19.6nm. The higher the annealing temperature is, the lower the micro-hardness of the alloy surface (100μm) is. When the annealing temperature is 250°C, the micro-hardness of the material is substantially no difference from that without the annealing process. When the treatment time of SMAT augments, the strain rate and the residual stress of Zr-4 alloy indicate an increasing trend, and the increase process is in rapid growth in the early stage and in slow growth in the later stage. After 60mins of treatment, the residual stress of Zr-4 alloy sample reaches 381.5MPa and the average micro-distortion is 0.42%.

1. Introduction

Surface nanocrystallization of alloy materials has been a new method of surface coating in recent years. Special physical and chemical methods are adopted to refine the grains of the alloy surface to nanoscale while retaining the relevant properties of the original material. Surface nanocrystallization of the material surface can effectively improve the properties of the material surface structure and increase its fatigue strength and corrosion resistance (Amarante et al., 2017; Li et al., 2016; Li et al., 2017; Lu et al., 2000; Lu and Lu, 2004; Nayak, 2016; Wen, Li and Rong, 2008; Li et al, 2015; Wang et al., 2015).

At present, surface mechanical lapping method (Huang et al., 2006), supersonic particle bombardment (Hou et al, 2008), cam roll-in method (Fan et al, 2005), shot peening method (Umemoto et al., 2005; Rafiee and Sadeghiazad, 2016) and other methods can make the surface of the material have a significantly plastic deformation in order to achieve surface nanocrystallization of the materials. Compared with other technologies, surface mechanical attrition treatment (SMAT) is featured with universality, high toughness, good combination with the interface, in favor of post-processing and other advantages. Currently, there have existed a number of related research (Sun et al., 2008; Sabirgalieva et al., 2017; Sun et al, 2008; Nai et al, 2003; Roland et al, 2006; Lu and Lu, 2004; Meyers et al., 2006; Tao et al, 1999).

The nanocrystallization of industrial Zr-4 alloy surface is realized by means of the mechanical grinding technology. XRD diffractometer and transmission electron microscopy are applied to analyze the grain size,

the microhardness and the microstructure of Zr-4 alloy at different annealing temperatures. Meanwhile, a X-ray stress gauge is adopted to measure the stress properties of Zr-4 alloy.

2. Test materials and test methods

The test sample is annealed Zr-4 alloy, and the other chemical components are Sn (1.1-1.7%), Fe (0.15-0.25%), Cr (0.08-0.12%) and Ni (<0.007%). Zr-4 alloy plate is cut apart into several samples of 80mm×85mm×3mm. Pretreatment is conducted on the sample, including decontamination, oil removal, grinding and drying. The relevant parameters of the surface mechanical attrition treatment (SMAT) are as follows: the system vibration frequency is 60Hz; the pellet material is GCr15; the diameter is 2mm. SMAT treatment time is set as 15mins, 30mins, 45mins and 60mins respectively.

XRD diffractometer is employed to measure the grain size of SMATed Zr-4 surface. The scanning angle is 20 to 80 degrees. The scanning speed is 3 degrees per minute. The tube current is 40mA. U-PMTVC light microscopy is adopted to measure the cross-sectional structure of the samples. The microstructures are analyzed at different depths by the JEM transmission electron microscopy. The etchants are $HF+8HNO_3+9H_2O$. XSTRESS stress gauge is applied to measure the residual stress of the sample along depth.

3. Test results and analysis

3.1 Effect of annealing temperature on grain size

Figure 1 illustrates the XRD diffraction pattern of the original sample at different SMAT treatment time. According to the figure, compared with the original sample, the diffraction characteristics of Zr-4 alloy after the SMAT treatment have changed significantly. The grain orientation in the SMAT treatment process experiences a transformation, and the diffraction peak intensity of the sample also accordingly changes. The diffraction peak of the treated sample shows the phenomenon of crystal face broadening. Meantime, with the increase of the annealing temperature, the diffraction peak of the sample becomes sharpened, that is, the microstrain decreases within the grain size in the annealing process.
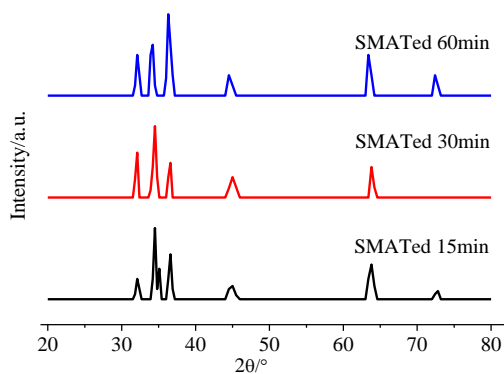
Figure 1: Bragg diffraction peak of XRD patterns for the SMATed Zr-4 alloy
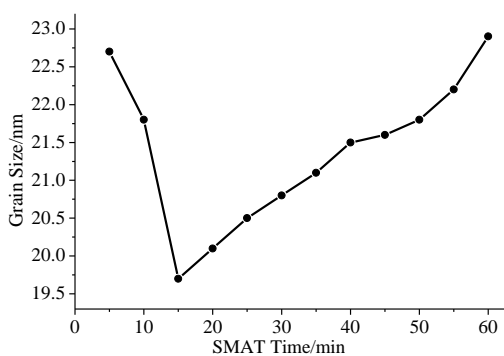
Figure 2: Change of the average grain size of the Zr-4 with SMAT time

Figure 2 indicates the relationship curve between the average size of the grains on Zr-4 alloy surface and SMAT treatment time. As seen from the figure, the average size of the grain on the Zr-4 alloy surface is 22.8nm when the mechanical lapping time is 5mins. As the SMAT treatment time lengthens, the size of the grain on the alloy surface tends to first drop and then increase. When the treatment time is 15mins, the grain size reaches a minimum of 19.6nm. The related research has confirmed that, as the strain force rises, the grain size is further reduced due to the increase of the dislocation density, but the increase of the deformation amount has no effect on the grain size. This is due to that the dislocation propagation and the annihilation rate maintain a dynamic equilibrium at a certain strain rate, and no new dislocation tangled structure emerges within the grain. Besides, when the SMAT treatment time is relatively long, the grain size extends instead, which is caused by the elevation of the temperature of the alloy surface.

3.2 Effect of annealing temperature on microhardness

Figure 3 indicates the relationship curve between the micro-hardness and the depth of alloy materials under four kinds of annealing temperatures. Based on the figure, generally speaking, the higher the annealing temperature is, the lower the microhardness of the alloy surface (100 μm) is. When the annealing temperature is 250°C, the microhardness of the material is almost no difference compared with that without annealing. When the annealing temperature exceeds 400°C, the hardness of the annealed material is significantly lower than that in the annealing process. When the annealing temperature is 250 °C, with the increase of the depth, the microhardness of the material rapidly drops and changes into the property of slow reduction of vibration. When the temperature exceeds 400°C, as the depth extends, the decreasing trend of the microhardness is not obvious, which is caused by the increase in the grain within the sample. The higher the temperature is, the greater the stress release amount within the grain is, which eases surface hardening.
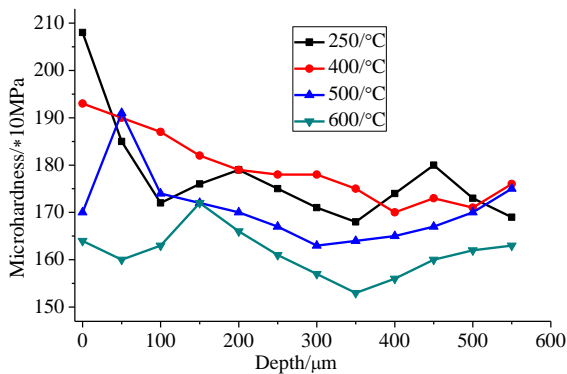
Figure 3: Microhardness variation along depth at different temperatures

3.3 An analysis on chemical stability of surface nanocrystallization of Zr-4 alloy

Figure 4 demonstrates the images of the microstructure of the nanostructured Zr-4 alloy surface after SMAT treatment for 30 mins and 50 mins. As seen from the figure, the grain on the alloy surface is in a continuous distribution. The twin crystal density within the alloy moves up with the increase of SMAT treatment time. In the figure, the microstructure, the grain size and the orientation and other key information of Zr-4 alloy are clearly observable. The space from the alloy surface to the inside of the matrix is divided into a completely deformed area, a transition zone and a matrix area. Specifically, the grains in the completely deformed area have all become fragmented. More twin crystals occur in the grain structure in the transition zone. The matrix area is mainly composed of equiaxed grains. The number and the distribution of twin crystals within Zr-4 alloy reflect the degree of plastic deformation of Zr during the surface mechanical treatment. Comparing Figure 4(a) and Figure 4(b), when the SMAT treatment time enlarges, the number and the density of twin crystals are gradually increasing. The Zr-4 alloy sample exhibits a structure of with a thickness of about 10μm, and its component parts are not yet known. After SMAT treatment, the surface crystals of Zr-4 alloy have been refined to nanoscale.

(a) 30min   (b) 50min
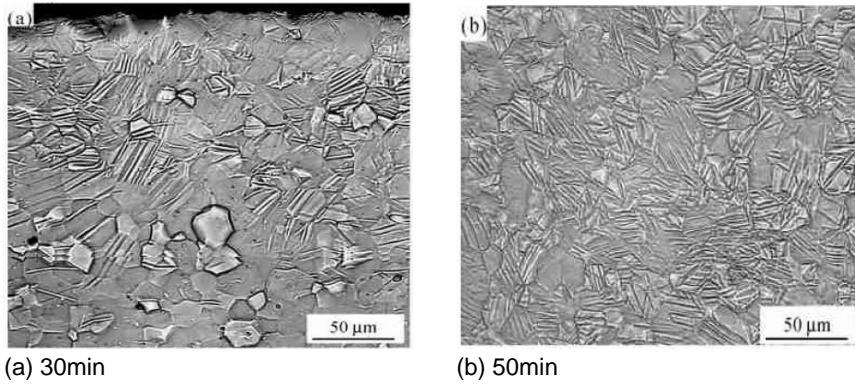
Figure 4: Cross-sectional deflection polarizing microstructures of the SNC CP-Zr for different time

3.4 The stress characteristics of Zr-4 alloy surface nanocrystallization

The lattice distortion and the residual stress of Zr-4 alloy treated by SMAT are calculated. The calculation results are illustrated in Figure 5. As seen from the figure, as the treatment time of SMAT extends, the strain rate and the residual stress of Zr-4 alloy surface show an increasing trend. Besides, in the increase process, rapid growth occurs in the early stage and slow growth happens in the latter stage. After 60mins of treatment, the residual stress of Zr-4 alloy sample is 381.5MPa and the average micro-distortion is 0.42%. This is due to that the mechanical lapping increasingly elevates the temperature of the alloy surface and the plastic deformation on the surface accordingly augments, which further leads to dynamic recovery and recrystallization.
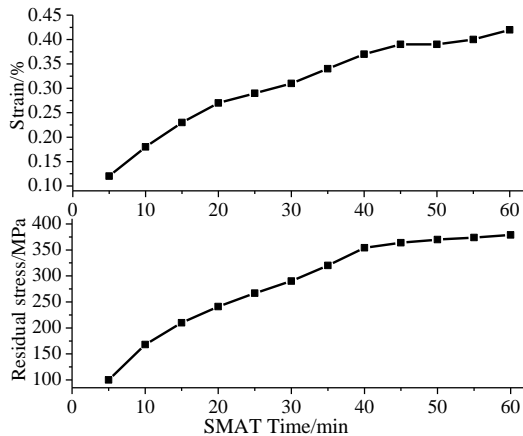
Figure 5: Strain and microcosmic residual stress of CP-Zr by SNC treatment

Figure 6 illustrates the residual stress property curve of Zr-4 alloy with the SMAT treatment time of 15 mins, 30 mins and 60 mins. In view of the figure, the residual compressive stress field appears in the strengthening layer after SMAT treatment, and the fatigue life of the material is further improved. Table 1 demonstrates the surface-related characteristic parameters of Zr-4 alloy under different processes. Specifically, σ_{srs} is the compressive stress on the surface of the material; σ_{mrs} is the maximum residual compressive stress; Z_m is the position and depth of the maximum residual compressive stress; Z_0 is the field depth of the residual compressive stress. Based on Figure 5 and Table 1, the σ_{srs} of the material is featured with a rise first and then a drop as the shot peening time prolongs, which is because the plastic deformation of the alloy surface continues to extend and the alloy surface temperature of the deformation layer gradually moves up. As a consequence, dynamic recovery and recrystallization occur to the material, and the residual compressive stress is released. Besides, σ_{mrs} tends to augment first and reduce then, and the maximum value of σ_{mrs} is -627MPa. The reason is that cyclic elastic-plastic deformation appears on the surface of the material during SMAT treatment, which further causes cyclic hardening. Z_m and Z_0 are proportional to the shot peening time.

Table 1: Characteristic parameters of compressive residual stress of CP-Zr

SMATed time/min	σ_{srs}/MPa	σ_{mrs}/MPa	Z_m/μm	Z_0/μm
15	-420.1	-505.4	114	277
30	-425.3	-619.3	183	381
45	-467.2	-626.8	190	385
60	-398.6	-622.5	206	434
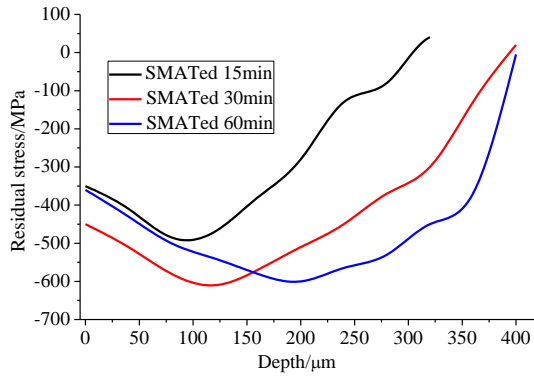
Figure 6: Macroscopic residual stress distribution of SNC CP-Zr with depth from surface

4. Conclusions

The nanocrystallization of the industrial Zr-4 alloy surface is realized by means of the mechanical lapping technology. XRD diffractometer and transmission electron microscopy are applied to analyze the grain size, the micro-hardness and the micro-structure of Zr-4 alloy at different annealing temperatures. Meanwhile, a X-ray stress gauge is adopted to measure the stress properties of Zr-4 alloy. The conclusions are as follows:

(1) Mechanical lapping technology can effectively realize the surface nanocrystallization of industrial zirconium, and Zr-4 alloy can form a gradient nanometer crystal structure on its surface after mechanical lapping.

(2) After SMAT processing, the diffraction characteristics of Zr-4 alloy have showed significant changes. The grain orientation has been transformed in the process of SMAT treatment and the diffraction peak intensity of the sample changes with the increase of SMAT treatment time. The size of the grain on the alloy surface tends to drop first and then rise. When the treatment time is 15mins, the grain size reaches a minimum value of 19.6nm.

(3) The higher the annealing temperature is, the lower the microhardness of the alloy surface (100 μm) is. When the annealing temperature is 250°C, the microhardness of the material is substantially no difference from that without the annealing process.

(4) When the treatment time of SMAT lengthens, the strain rate and the residual stress of Zr-4 alloy surface demonstrate an upward trend. In the increase process, rapid growth occurs in the early stage and it slows down in the latter stage. After 60mins of treatment, the residual stress of the Zr-4 alloy sample is 381.5MPa and the average micro-distortion is 0.42%.

Acknowledgment

References

Amarante T.A., Silva S.C., Almeida Neto A.F., 2017, Influence assessment of operating parameters in synthesis of zn-ni alloys for process electrodeposition, Chemical Engineering Transactions, 57, 1651-1656, DOI: 10.3303/CET1757276

Fan X., Zhou B., Zhu L., Wang H., Huang J., 2005, Surface Nanocrystallization of Low Carbon Steel Induced by Circulation Rolling Plastic Deformation, Materials Science Forum 475-479, 133-136. DOI: 10.4028/www.scientific.net/msf.475-479.133.

Hou L., Wei Y., Liu B., Xu B., 2008, High energy impact techniques application for surface grain refinement in az91d magnesium alloy, Journal of Materials Science, 43(13), 4658-4665. DOI: 10.1007/s10853-008-2668-0.

Huang L., Lu J., Troyon M., 2006, Nanomechanical properties of nanostructured titanium prepared by smat, Surface & Coatings Technology, 201, 1-2, 208-213. DOI: 10.1016/j.surfcoat.2005.11.090.

Li S., Zhang Y., Li Y., Liao R., 2015, Equilibrium calculation and technological parameters optimization of natural gas liquefaction process with mixed refrigerant, International Journal of Heat and Technology, 33(2), 123-128, DOI: 10.18280/ijht.330220.

Li X., Tang C., Wang Q., Li X.P., Hao J., 2017, Molecular simulation research on the micro effect mechanism of interfacial properties of nano SiO2/meta-aramid fiber, International Journal of Heat and Technology, 35(1), 123-129, DOI: 10.18280/ijht.350117

Li Y., Zhang Y.X., Kong X.R., Ding Y.P., Zhang R.Z., Tang J.Y., 2016, Thermal stability of the Mg2Ni-based hydrogen storage alloy doped Ti element, International Journal of Heat and Technology, 34(2), 245-250, DOI: 10.18280/ijht.340213

Lu K., Lu J., 2004, Nanostructured surface layer on metallic materials induced by surface mechanical attrition treatment, Materials Science & Engineering A, s 375-377, 1, 38-45. DOI: 10.1016/j.msea.2003.10.261.

Lu L., Sui M., Lu K., 2000, Superplastic extensibility of nanocrystalline copper at room temperature, Science, 287, 5457, 1463. DOI: 10.1126/science.287.5457.1463.

Meyers M.A., Mishra A., Benson D.J., 2006, The deformation physics of nanocrystalline metals: experiments, analysis, and computations, JOM, 58(4), 41-48, DOI: 10.1007/s11837-006-0214-6.

Nai R., Wei P., Zhen B., 2003, Mechanical and wear properties of nanostructured surface layer in iron induced by surface mechanical attrition treatment. Journal of Materials Science & Technology, 19(6), 563-566, DOI: 10.4028/www.scientific.net/kem.353-358.1810.

Nayak M.K., 2016, Wire coating analysis in MHD flow and heat transfer of a third-grade fluid with variable viscosity in a porous medium with internal heat generation/absorption and joule heating, Modelling, Measurement and Control B, 85(1), 105-122.

Rafiee S., Sadeghiazad M., 2016, Heat and mass transfer between cold and hot vortex cores inside ranque-hilsch vortex tube-optimization of hot tube length, International Journal of Heat and Technology, 34(1), 31-38, DOI: 10.18280/ijht.340105.

Roland T., Retraint D., Lu K., Lu J., 2006, Fatigue life improvement through surface nanostructuring of stainless steel by means of surface mechanical attrition treatment. Scripta Materialia, 54, 11, 1949-1954. DOI: 10.1016/j.scriptamat.2006.01.049.

Sabirgalieva N., Skartlien R., Rojas-Solorzano L., 2017, Dpd simulation of surface wettability alteration by added water-soluble surfactant in the presence of indigenous oil-soluble surfactant, Chemical Engineering Transactions, 57, 1489-1494, DOI: 10.3303/CET1757249

Sun H., Shi Y., Zhang M., 2008, Wear behaviour of az91d magnesium alloy with a nanocrystalline surface layer. Surface & Coatings Technology, 202(13), 2859-2864, DOI: 10.1016/j.surfcoat.2007.10.025.

Sun H., Shi Y., Zhang M., Lu K., 2008, Surface alloying of an mg alloy subjected to surface mechanical attrition treatment, Surface & Coatings Technology, 202(16), 3947-3953, DOI: 10.1016/j.surfcoat.2008.02.010.

Tao N., Sui M., Lu J., Lua K., 1999, Surface nanocrystallization of iron induced by ultrasonic shot peening, Nanostructured Materials, 11(4), 433-440, DOI: 10.1016/s0965-9773(99)00324-4.

Umemoto M., Todaka Y., Tsuchiya K., 2005, Formation of nanocrystalline structure in steels by air blast shot peening, Materials Transactions, 44(7), 1488-1493. DOI: 10.2320/matertrans.44.1488.

Wang J.T. Yu W.L., Wang T., Wang Y.L., Gao Y.L., 2015, First-principles study on the thermodynamic defect and crystal structure of U-12.5 at% Nb alloy, International Journal of Heat and Technology, 33(1), 175-180, DOI: 10.18280/ijht.330124

Wen C., Li W., Rong Y., 2008, Nanocrystallization and martensitic transformation in fe-23.4mn-6.5si-5.1cr (wt.%) alloy by surface mechanical attrition treatment, Materials Science & Engineering A, s 481-482, 1, 484-488, DOI: 10.1016/j.msea.2007.03.125.